IOPs using a normal curve was 18.8 mmHg. IOP over 18.8 mmHg was regarded here as elevated IOP.
Found at: doi:10.1371/journal.pone.0009050.s002 (0.57 MB TIF)

Figure S3 Anti-myocilin staining of trabecular meshwork in Vav2/Vav3-deficient mice. Immunohistochemical staining of trabecular meshwork with anti-myocilin antibody in representative iridocorneal angle sections of age-matched wild-type and Vav2/Vav3-deficient ($Vav2^{-/-}Vav3^{-/-}$) 7-week-old mice with normal IOP, with either evidence of angle closure, or normal open angles similar to wild type mice. Myocilin (green-labeled), which is strongly expressed in TM cells, was regarded as a marker for TM cells. In $Vav2^{-/-}Vav3^{-/-}$ mice with angle closure, myocilin was not detected in the iridocorneal angle (indicated by arrows). Conversely, it was detected in sections from mice with normal open angles, similar to those in wild type mice. Blue fluorescence is DAPI counter staining. Scale bars, 20 um.
Found at: doi:10.1371/journal.pone.0009050.s003 (2.19 MB TIF)

Figure S4 Effects of ocular hypotensives in Vav2/Vav3-deficient mice. A. Ocular hypotensives used for human glaucoma, latanoprost, a prostaglandin analogue was tested in 7-week-old Vav2/Vav3-deficient ($Vav2^{-/-}Vav3^{-/-}$) mice with elevated IOP ($n = 20$). The IOP was measured 3 hours before and after topical application of 3 µl of 0.01% latanoprost in a masked manner. Vehicle was used as a control. Latanoprost lowered the IOP significantly in $Vav2^{-/-}Vav3^{-/-}$ mice (26.3 ± 5.0 mmHg versus 15.8 ± 5.1 mmHg; $n = 20$), while the IOP was not altered by the vehicle alone. The latanoprost-induced reduction of IOP in $Vav2^{-/-}Vav3^{-/-}$mice was statistically significant (**$P<0.01$, $n = 20$). The data shown are representative of three independent experiments performed. Error bars represent S.D. **$P<0.01$ versus vehicle-treated $Vav2^{-/-}Vav3^{-/-}$ mice. B. Using three different drugs for lowering IOP, we compared the effects by percentages of elevated IOP reduction. These data are representative from three independent experiments, respectively ($n = 20$). Error bars represent S.D. **$P<0.01$ versus vehicle-treated $Vav2^{-/-}Vav3^{-/-}$ mice. C. Rho-associated protein kinase Inhibitor, Y-27632 was tested for lowering IOP on $Vav2^{-/-}Vav3^{-/-}$ mice ($n = 20$). Y27632 administration has no effect against $Vav2^{-/-}Vav3^{-/-}$ mice (before, 19.69 ± 4.98 mmHg; after, 18.83 ± 5.60 mmHg; $n = 20$), while Y-27632 lowered the IOP significantly in age-matched wild-type mice (13.58 ± 2.27 mmHg versus 12.31 ± 1.94 mmHg; $n = 20$. $p<0.05$) and the IOP was not altered by the vehicle solution (13.25 ± 1.71 mmHg versus 13.18 ± 3.17 mmHg; $n = 20$). These data are representative from four independent experiments, respectively. Error bars represent S.D. *$P<0.05$ versus vehicle-treated WT mice.
Found at: doi:10.1371/journal.pone.0009050.s004 (0.41 MB TIF)

Figure S5 Sense probe staining for in situ hybridization experiments in ocular tissues. In situ hybridization with Vav2 and Vav3 sense probes were carried out as negative controls for the experiments. C57BL/6 mouse ocular tissue sections including the iridocorneal angle, sclera and cornea were used. With sense probes, there was no detectable signal around mouse iridocorneal angle tissues. TM; trabecular meshwork. Scl; sclera.
Found at: doi:10.1371/journal.pone.0009050.s005 (4.14 MB TIF)

Acknowledgments

The authors thank Professor Duco Hamasaki (Bascom Palmer Eye Institute, University of Miami School of Medicine, Florida) and Morton Smith, M.D. (Washington University Department of Ophthalmology & Visual Sciences) for helpful suggestions and discussion; and Mr. Tsutomu Osanai and Ms. Takae Oyama for technical help.

Author Contributions

Conceived and designed the experiments: KF TI KI. Performed the experiments: KF TI MA HK MF QC. Analyzed the data: KF TI KI MA MF MW EMB WAS. Contributed reagents/materials/analysis tools: KF TI KI MW WAS. Wrote the paper: KF KI EMB WAS.

References

1. Kass MA, Heuer DK, Higginbotham EJ, Johnson CA, Keltner JL, et al. (2002) The ocular hypertension treatment study: a randomized trial determines that topical ocular hypotensive medication delays or prevents the onset of primary open-angle glaucoma. Arch Ophthalmol 120: 701–713.
2. AGIS investigators (2002) The advanced glaucoma intervention study (AGIS): 7. The relationship between control of intraocular pressure and visual field deterioration. Am J Ophthalmol 130: 429–440.
3. Gabelt BT, Kaufman PL (2005) Changes in aqueous humor dynamics with age and glaucoma. Prog Retin Eye Res 24: 612–637.
4. Tan JC, Peters DM, Kaufman PL (2006) Recent developments in understanding the pathophysiology of elevated intraocular pressure. Curr Opin Ophthalmol 17: 168–174.
5. Bustelo XR (2001) Vav protein, adaptors and cell signaling. Oncogene 20: 6372–6381.
6. Schmidt A, Hall A (2002) Guanine nucleotide exchange factors for Rho GTPases: turning on the switch. Genes Dev 16: 1587–1609.
7. Turner M, Billadeau DD (2002) VAV proteins as signal integrators for multi-subunit immune-recognition receptors. Nat Rev Immunol 2: 476–486.
8. Swat W, Fujikawa K (2005) The Vav family: at the crossroads of signaling pathways. Immunol Res 32: 259–265.
9. Riteau B, Barber DF, Long EO (2003) Vav1 phosphorylation is induced byβ2 integrin engagement on natural killer cells upstream of actin cytoskeleton and lipid raft reorganization. J Exp Med 198: 469–474.
10. Gakidis MAM, Cullere X, Olson T, Wilsbacher JL, Zhang B, et al. (2004) Vav GEFs are required for β2 integrin-dependent functions of neutrophils. J Cell Biol 166: 273–282.
11. Holsinger LJ, Graef IA, Swat W, Chi T, Bautista DM, et al. (1998) Defects in actin-cap formation in Vav-deficient mice implicate an actin requirement for lymphocyte signal transduction. Curr Biol 8: 563–572.
12. Cella M, Fujikawa K, Tassi I, Kim S, Latinis K, et al. (2004) Differential requirements for Vav proteins in DAP10- and ITAM-mediated NK cell cytotoxicity. J Exp Med 200: 817–823.
13. Doody GM, Bell SE, Vigorito E, Clayton E, McAdam S, et al. (2001) Signal transduction through Vav-2 participates in humoral immune responses and B cell maturation. Nat Immunol 2: 542–547.
14. Faccio R, Teitelbaum SL, Fujikawa K, Chappel J, Zallone A, et al. (2005) Vav3 regulates osteoclast function and bone mass. Nat Med 11: 284–290.
15. Fujikawa K, Miletic AV, Alt FW, Faccio R, Brown T, et al. (2003) Vav1/2/3-null mice define an essential role for Vav family proteins in lymphocyte development and activation but a differential requirement in MAPK signaling in T and B cells. J Exp Med 198: 1595–1608.
16. Tybulewicz VLJ, Ardouin L, Prisco A, Reynolds LF (2003) Vav1: a key signal transducer downstream of the TCR. Immunol Rev 192: 42–52.
17. Karali A, Russell P, Stefani FH, Tamm ER (2000) Localization of myocilin/trabecular meshwork-inducible glucocorticoid response protein in the human eye. Invest Ophthalmol Vis Sci 41: 729–740.
18. Weinreb RN, Toris CB, Gabelt BT, Lindsey JD, Kaufman PL (2002) Effects of prostaglandins on the aqueous humor outflow pathways. Surv Ophthalmol 47 (suppl. 1): S53–S64.
19. Neufeld AH (1979) Experimental studies on the mechanism of action of timolol. Surv Ophthalmol 23: 363–370.
20. Pfeiffer N (1997) Dorzolamide: Development and clinical application of a topical carbonic anhydrase inhibitor. Surv Ophthalmol 42: 137–151.
21. Tanihara H, Inatani M, Honjo M, Tokushige H, Azuma J, et al. (2008) Intraocular pressure-lowering effects and safety of topical administration of a selective ROCK inhibitor, SNJ-1656, in healthy volunteers. Arch Ophthalmol 126: 309–315.
22. Rao PV, Peterson YK, Inoue T, Casey PJ (2008) Effects of pharmacologic inhibition of protein geranylgeranyltransferase type I on aqueous humor outflow through the trabecular meshwork. Invest Ophthalmol Vis Sci 49: 2464–2471.
23. Honjo M, Tanihara H, Inatani M, Kido N, Sawamura T, et al. (2001) Effects of Rho-associated protein kinase inhibitor, Y-27632, on intraocular pressure and outflow facility. Invest Ophthalmol Vis Sci 42: 137–144.
24. Pang IH, Clark AF (2007) Rodent models for glaucoma retinopathy and optic neuropathy. J Glaucoma 16: 483–505.
25. Aihara M, Lindsey JD, Weinreb RN (2003) Aqueous humor dynamics in mice. Invest Ophthalmol Vis Sci 44: 5168–5173.
26. Chang B, Smith RS, Hawes NL, Anderson MG, Zabaleta A, et al. (1999) Interacting loci cause severe iris atrophy and glaucoma in DBA/2J mice. Nat Genet 21: 405–409.

27. John SW, Smith RS, Savinova OV, Hawes NL, Chang B, et al. (1998) Essential iris atrophy, pigment dispersion, and glaucoma in DBA/2J mice. Invest Ophthalmol Vis Sci 39: 951–962.
28. Goldblum D, Kipfer-Kauer A, Sarra GM, Wolf S, Frueh BE (2007) Distribution of amyloid precursor protein and amyloid-beta immunoreactivity in DBA/2J glaucomatous mouse retinas. Invest Ophthalmol Vis Sci 48: 5085–5090.
29. Schlamp CL, Li Y, Dietz JA, Janssen KT, Nickells RW (2006) Progressive ganglion cells loss and optic nerve degeneration in DBA/2J mice is variable and asymmetric. BMC Neurosci 7: 66.
30. Anderson MG, Smith RS, Hawes NL, Zabaleta A, Chang B, et al. (2002) Mutations in genes encoding melanosomal proteins cuase pigmentary glaucoma in DBA/2J mice. Nat Genet 1: 81–85.
31. Nakano M, Ikeda Y, Taniguchi T, Yagi T, Fuwa M, et al. (2009) Three susceptible loci associated with primary open-angle glaucoma identified by genome-wide association study in a Japanese population. Proc Natl Acad Sci U S A 106(31): 12838–12842.
32. Tanito M, Minami M, Akahori M, Kaidzu S, Takai Y, et al. (2008) LOXL1 variants in elderly Japanese patients with exfoliation syndrome/glaucoma, primary open-angle glaucoma, normal tension glaucoma, and cataract. Mol Vis 14: 1898–1905.
33. Shibuya E, Meguro A, Ota M, Kashiwagi K, Mabuchi F, et al. (2008) Association of Toll-like receptor 4 gene polymorphisms with normal tension glaucoma. Invest Ophthalmol Vis Sci 49: 4453–4457.
34. Funayama T, Mashima Y, Ohtake Y, Ishikawa K, Fuse N, et al. (2006) SNPs and interaction analyses of noelin 2, myocilin, and optineurin genes in Japanese patients with open-angle glaucoma. Invest Ophthalmol Vis Sci 47: 5368–5375.
35. Inagaki Y, Mashima Y, Fuse N, Funayama T, Ohtake Y, et al. (2006) Polymorphism of b-adrenergic receptors and susceptibility to open-angle glaucoma. Mol Vis 12: 673–680.
36. Ishikawa K, Funayama T, Ohtake Y, Kimura I, Ideta H, et al. (2005) Association between glaucoma and gene polymorphism of endothelin type A receptor. Mol Vis 11: 431–437.
37. Jiao X, Yang Z, Yang X, Chen Y, Tong Z, et al. (2009) Common variants on chromosome 2 and risk of primary open-angle glaucoma in the Afro-Caribbean population of Barbados. Proc Natl Acad Sci U S A 106(40): 17105–17110.
38. Wolf C, Gramer E, Müller-Myhsok B, Pasutto F, Reinthal E, et al. (2009) Evaluation of nine candidate genes in patients with normal tension glaucoma: a case control study. BMC Med Genet 10: 91.
39. Narooie-Nejad M, Paylakhi SH, Shojaee S, Fazlali Z, Rezaei Kanavi M, et al. (2009) Loss of function mutations in the gene encoding latent transforming growth factor beta binding protein 2, LTBP2, cause primary congenital glaucoma. Hum Mol Genet 18(20): 3969–3977.
40. Sud A, Del Bono EA, Haines JL, Wiggs JL (2008) Fine mapping of the GLC1K juvenile primary open-angle glaucoma locus and exclusion of candidate genes. Mol Vis 4: 1319–1326.
41. Liu Y, Schmidt S, Qin X, Gibson J, Hutchins K, et al. (2008) Lack of association between LOXL1 variants and primary open-angle glaucoma in three different populations. Invest Ophthalmol Vis Sci 49(8): 3465–3468.
42. Thorleifsson G, Magnusson KP, Sulem P, Walters GB, Gudbjartsson DF, et al. (2007) Common sequence variants in the LOXL1 gene confer susceptibility to exfoliation glaucoma. Science 317(5843): 1397–1400.
43. Kumar A, Basavaraj MG, Gupta SK, Qamar I, Ali AM, et al. (2007) Role of CYP1B1, MYOC, OPTN, and OPTC genes in adult-onset primary open-angle glaucoma: predominance of CYP1B1 mutations in Indian patients. Mol Vis 13: 667–676.
44. Bill A, Svedberg B (1972) Scanning electron microscopic studies of the trabecular meshwork and the canal of Schlemm: an attempt to localize the main resistance to outflow of aqueous humor in man. Acta Ophthalmol 50: 295–320.
45. Wiedelholt M, Bielka S, Schweig F, Lütjen-Drecoll E, Lepple-Wienhues A (1995) Regulation of outflow rate and resistance in the perfused anterior segment of the bovine eye. Exp Eye Res 61: 223–234.
46. Filla MS, Woods A, Kaufman PL, Peters DM (2006) Beta1 and beta3 integrins cooperate to induce syndecan-4-containing cross-linked actin networks in human trabecular meshwork cells. Invest Ophthalmol Vis Sci 47(5): 1956–1967.
47. Peterson JA, Sheibani N, David G, Garcia-Pardo A, Peters DM (2005) Heparin II domain of fibronectin uses alpha4beta1 integrin to control focal adhesion and stress fiber formation, independent of syndecan-4. J Biol Chem 25 280(8): 6915–6922.
48. Diskin S, Cao Z, Leffler H, Panjwani N (2009) The role of integrin glycosylation in galectin-8-mediated trabecular meshwork cell adhesion and spreading. Glycobiology 19(1): 29–37.
49. Fukaya M, Hayashi Y, Watanabe M (2005) NR2 to NR3B subnit switchover of NMDA receptors in early postnatal motoneurons. Eur J Neurosci 21: 1432–1436.

HMG Advance Access published April 28, 2010

Human Molecular Genetics, 2010 **1–10**
doi:10.1093/hmg/ddq146

Overexpression of optineurin E50K disrupts Rab8 interaction and leads to a progressive retinal degeneration in mice

Zai-Long Chi[1,†], Masakazu Akahori[1,†], Minoru Obazawa[1], Masayoshi Minami[1], Toru Noda[1], Naoki Nakaya[2], Stanislav Tomarev[2], Kazuhide Kawase[3], Tetsuya Yamamoto[3], Setsuko Noda[4], Masaki Sasaoka[5], Atsushi Shimazaki[5], Yuichiro Takada[1] and Takeshi Iwata[1,*]

[1]National Institute of Sensory Organs, National Hospital Organization Tokyo Medical Center, 2-5-1 Higashigaoka, Meguro-ku, Tokyo 152-8902, Japan, [2]National Eye Institute, National Institutes of Health, 5635 Fishers Lane, Room 1124, Rockville, MD 20852, USA, [3]Department of Ophthalmology, Gifu University Graduate School of Medicine, 1-1 Yanagido, Gifu 501-1194, Japan, [4]Department of Nursing, Tokai University School of Health Sciences, Boseidai, Isehara, Kanagawa Prefecture 259-1193, Japan and [5]Research & Development Center, Santen Pharmaceutical Co., Ltd, 8916-16, Takayama-cho, Ikoma, Nara Prefecture 630-0101, Japan

Received March 16, 2010; Revised and Accepted April 12, 2010

Glaucoma is one of the leading causes of bilateral blindness affecting nearly 8 million people worldwide. Glaucoma is characterized by a progressive loss of retinal ganglion cells (RGCs) and is often associated with elevated intraocular pressure (IOP). However, patients with normal tension glaucoma (NTG), a subtype of primary open-angle glaucoma (POAG), develop the disease without IOP elevation. The molecular pathways leading to the pathology of NTG and POAG are still unclear. Here, we describe the phenotypic characteristics of transgenic mice overexpressing wild-type (Wt) or mutated optineurin (Optn). Mutations E50K, H486R and Optn with a deletion of the first (amino acids 153–174) or second (amino acids 426–461) leucine zipper were used for overexpression. After 16 months, histological abnormalities were exclusively observed in the retina of E50K mutant mice with loss of RGCs and connecting synapses in the peripheral retina leading to a thinning of the nerve fiber layer at the optic nerve head at normal IOP. E50K mice also showed massive apoptosis and degeneration of entire retina, leading to approximately a 28% reduction of the retina thickness. At the molecular level, introduction of the E50K mutation disrupts the interaction between Optn and Rab8 GTPase, a protein involved in the regulation of vesicle transport from Golgi to plasma membrane. Wt Optn and an active GTP-bound form of Rab8 complex were localized at the Golgi complex. These data suggest that alternation of the Optn sequence can initiate significant retinal degeneration in mice.

INTRODUCTION

Glaucoma is characterized by progressive loss of retinal ganglion cells (RGCs), degeneration of axons in the optic nerve and visual field defects. Primary open-angle glaucoma (POAG) is one of the major causes of irreversible blindness leading to vision loss in about 4.5 million people and accounting for 12% of global blindness (1,2). POAG is often associated with elevated intraocular pressure (IOP), which is one of main risk factors in glaucoma. However, degenerative changes in the RGC and the optic nerve head leading to progressive visual field loss may occur even in the absence of elevated IOP in a subtype of POAG called normal tension glaucoma (NTG). A recent epidemiological study in Tajimi,

*To whom correspondence should be addressed. Tel/Fax: +81 334111026; Email: iwatatakeshi@kankakuki.go.jp
†The first two authors contributed equally to this work.

Japan, demonstrated that >90% of POAG cases were diagnosed as NTG (3).

At least 24 different genetic loci have been linked to various forms of glaucoma, and four glaucoma-associated genes, *myocilin*, *cytochrome P4501B1*, *OPTN* and *WD repeat domain 36* (*WDR36*) have been previously identified (4–7). A significantly higher frequency of *OPTN* sequence alternations in glaucoma subjects compared with controls supports the contribution of this gene to the development of glaucoma (8–10). In one original report, >16.7% of NTG families had mutations in the *OPTN* gene (6), and a number of disease-causing amino acid substitutions including E50K, H486R and R545Q have been confirmed by others (8–10). The substitution of glutamic acid by lysine at amino acid 50 (E50K) is exclusively associated with familial and sporadic forms of NTG (6,8,11). We also identified E50K mutation in an NTG family in Japan (Supplementary Material 1). Several lines of evidence support E50K mutation could play a critical role for the severity of phenotype and pathology of glaucoma. Clinical study revealed that an NTG phenotype is more severe in subjects with the E50K mutation than in a control group of subjects with NTG but without this mutation, supporting a critical role for this mutation (8,12). *In vitro* cell biological study demonstrated that transfection of E50K-mutated optineurin (Optn) caused cell death of rat RGC cell line, RGC5 (13).

OPTN corresponds to the *GLC1E* locus for adult-onset POAG and is located in the 10p14 region. The *OPTN* gene contains 3 non-coding exons followed by 13 exons encoding a 577 amino acid protein. Almost all of the reported disease-causing mutations correspond to positions that are evolutionarily conserved between the mouse, monkey and human. OPTN is ubiquitously expressed in all tissues and interacts with number of proteins including huntingtin (14), transcription factor IIIA (15), Rab8 (16,17), myosin VI (18), FOS (19), ring finger protein 11 (20) and metabotrophic glutamate receptor 1-a (21), suggesting multiple cellular functions. Recent studies have shown that the *OPTN* promoter is induced by TNF-α (22). OPTN may function as an adaptor which regulates the assembly of TAX1BP1 and the post-translationally modified form of Tax1, leading to a sustained NF-κB activation (23).

The molecular pathways leading to glaucoma from a single gene mutation still remain unclear mainly due to (i) insufficiency of clinical and genetic information from glaucoma patients, (ii) difficulty in obtaining clinical material, such as optic nerve tissues, from patients and (iii) lack of animal models with particular gene mutations. Recently, it has been reported that glutamate transporter-deficient mice exhibit an NTG-like phenotype (24). However, to this date, no animal models have been produced based on the gene mutation found in NTG patients.

In this paper, we developed five variants of *Optn* overexpressing mice including the wild-type (Wt), E50K and H486R point mutants, and mutants with a deletion of the first or second leucine zipper. We used histopathology to investigate changes in the optic nerve and retina of each mutant. Using a modified protein fragment complementation method, we also investigated the effects of the E50K mutation on the interaction with OPTN-interacting protein Rab8, which controls the vesicle transport.

RESULTS

Construction of mouse Optn mutants and characterization of expression

Five mouse Optn variants were overexpressed under the CMV early enhancer/chicken beta-actin (CAG) promoter in transgenic mice. These variants included Wt Optn, the E50K and H489R mutants which are mouse equivalents of the human glaucoma-causing mutations E50K and H486R, respectively, and mutants with deletion of the first (1st LZ del) or second (2nd LZ del) Optn leucine zipper domain. All transgenic mice were born at normal Mendelian ratios, weighed the same as non-transgenic littermates and appeared normal up to 16 months of age. The mutant HA-tagged proteins were ubiquitously expressed in the entire retina (Fig. 1B). The copy numbers for each mutant cDNA construct were approximately 12 to 14 per mouse as determined by TaqMan real-time PCR assay (data not shown).

Comparison of histological changes in the eye of Wt and mutant Optn transgenic mice

Loss of RGCs and cupping of the optic disc are the defining histological features of the retina of patients with POAG and NTG. Therefore, we examined the eyes of aged Wt, E50K, H489R, 1st LZ del and 2nd LZ del mice using histology and immunohistochemistry. Cornea, lens and anterior segment of Wt and transgenic mice were histologically normal even in 16-month-old mice. For statistical analysis, measurements of retinal thickness were made at the peripheral retina ~1.0–1.2 mm from the optic nerve head. Remarkably, we found significant phenotypical changes in five independent transgenic mouse lines expressing the E50K mutant (Fig. 2A). The retinal thickness of E50K mice was significantly reduced compared with Wt mice at 16 months of age ($^*P < 0.05$) (Fig. 2B), but a reduction of the retinal thickness was observed as early as 12 months of age (Fig. 2C). Owing to the loss of RGCs and their axons in the peripheral retina, β-III tubulin-stained nerve fiber layer was relatively thinner at the optic nerve head of E50K mice compared with Wt mice (Fig. 2D). The anti-SMI32 immunostaining of the whole-mounted retina demonstrated loss of large RGCs in the peripheral retina (Fig. 2D). Progressive, non-specific loss of RGCs in E50K mice was shown by counting NeuN-stained cells in the entire retina sections (Fig. 2D).

To determine which retinal cell types are vulnerable to the E50K mutation, we performed immunohistochemical analysis using retinal cell-specific markers. Immunostaining with calretinin antibodies was used to visualize synapses of RGCs and amacrine cells in the inner plexiform layer of 16-month-old Wt and E50K mice (Fig. 3A). Although there was no difference in the immunolabeling pattern of synapses in the central retina of Wt and E50K mice (Box C**), a significant degeneration of synapses was observed in the peripheral retina of E50K mice versus Wt mice (Box P**). Immunolabeling of the flat mount retina using antibodies against choline acetyltransferase (ChAT, cholinergic amacrine) revealed areas of amacrine cell loss in the peripheral retina (Box P**) (Fig. 3B, arrow). Loss and/or changes of another type of amacrine cells and rod bipolar cells in the peripheral retina of

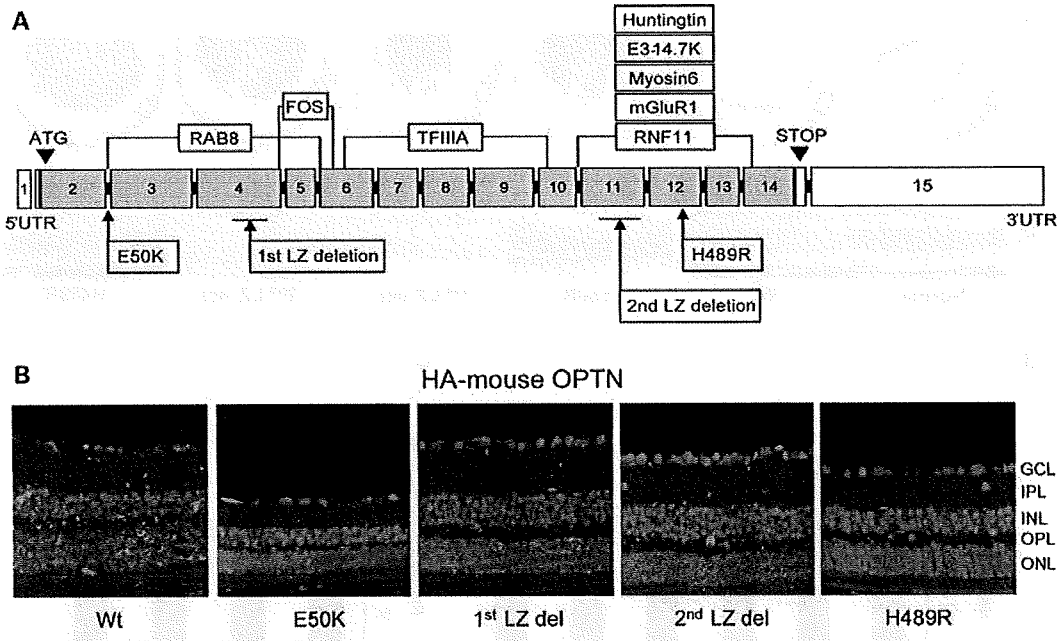

Figure 1. (A) Schematic diagram of the mouse Optn constructs used in this study. Positions of mutations and deletions are shown in lower boxes. Predicted binding sites of Optn-interacting proteins are shown in upper boxes. (B) Expression of Optn mutants in the retina of transgenic mice. Sections were immunostained with anti-HA antibody. Scale bar: 20 μm.

E50K mice versus Wt were detected by staining with antibodies against tyrosine hydroxylase (red, doperminergic amacrine cell) and PKC α (green, rod bipolar cell) (Fig. 3C, Box P**). The outer plexiform layer (OPL) and outer nuclear layer (ONL) were also affected in E50K mice. In the OPL, expression of synaptophysin, synaptic vesicle marker at the photoreceptor synaptic terminal, was reduced in E50K mice compared with Wt mice (Fig. 4), whereas rhodopsin-labeled outer segments were shorter in E50K mutant than in Wt mice.

Apoptosis assay by single-stranded DNA immunohistochemistry

RGC death by apoptosis is one of the typical features of glaucoma pathogenesis. Immunostaining with antibodies against single-stranded DNA (ssDNA), a marker of apoptosis-associated DNA damage, was used to detect apoptotic changes in the retina of E50K mice. ssDNA-positive (apoptotic) cells were detected not only in the RGCL (Fig. 4A, Arrow) but also in the INL and ONL. At the peripheral retina, significant increase of apoptotic cell number in all retinal layers was observed in E50K mice at 16 months of age (Fig. 4B) compared with age-matched Wt mice ($^{**}P < 0.01$).

IOP of Wt and mutant *Optn* transgenic mice

IOP measurement is a necessary and important step to determine whether retinal degeneration in our transgenic mice is associated with the elevation of IOP or it is IOP independent. IOP was measured using an impact-rebound tonometer and an optical interferometry tonometer. The average IOP reading from both devices gave similar IOP for mutant and Wt mice in the normal range of 15 ± 1 mmHg for all examined ages (Fig. 5). These results demonstrated that pathological features of E50K mice are not due to changes in IOP.

E50k mutation disrupts OPTN–Rab8 direct protein interaction

Protein–protein interaction of OPTN and Rab8 was analyzed after transfection of RGC5 or COS1 cells with constructs encoding OPTN (Wt, E50K), Rab8 [Wt, T22N (inactive GDP form) and Q67L (active GTP form)] tagged with fluorescent labels (Fig. 6A). We observed >4-fold decrease in the interaction between OPTN Wt and the active form (Q67L) versus the inactive form (T22N) of Rab8. However, E50K did not interact with either form of Rab8 in RGC5 cells (Fig. 6B). Interaction of Wt OPTN and the active form Rab8 was further supported by co-localization of the complex with a specific Golgi marker, GM130, in COS1 cells (Fig. 6C).

DISCUSSION

In the present study, we produced and characterized the phenotype of five different transgenic *Optn* mice lines including lines with overexpression of two *OPTN* mutations identified in glaucoma patients. Among the 15 *OPTN* mutations previously identified (P16A, H26D, E50K, K66R, E92V, E103D, 2 bp insertion between amino acids 127–128, V161M, H228Y, A336G, A377T, I407T, A466S, H486R and R545Q), we selected two mutations E50K and H486R, which has been confirmed by several groups to be associated with severe NTG and/or juvenile open-angle glaucoma

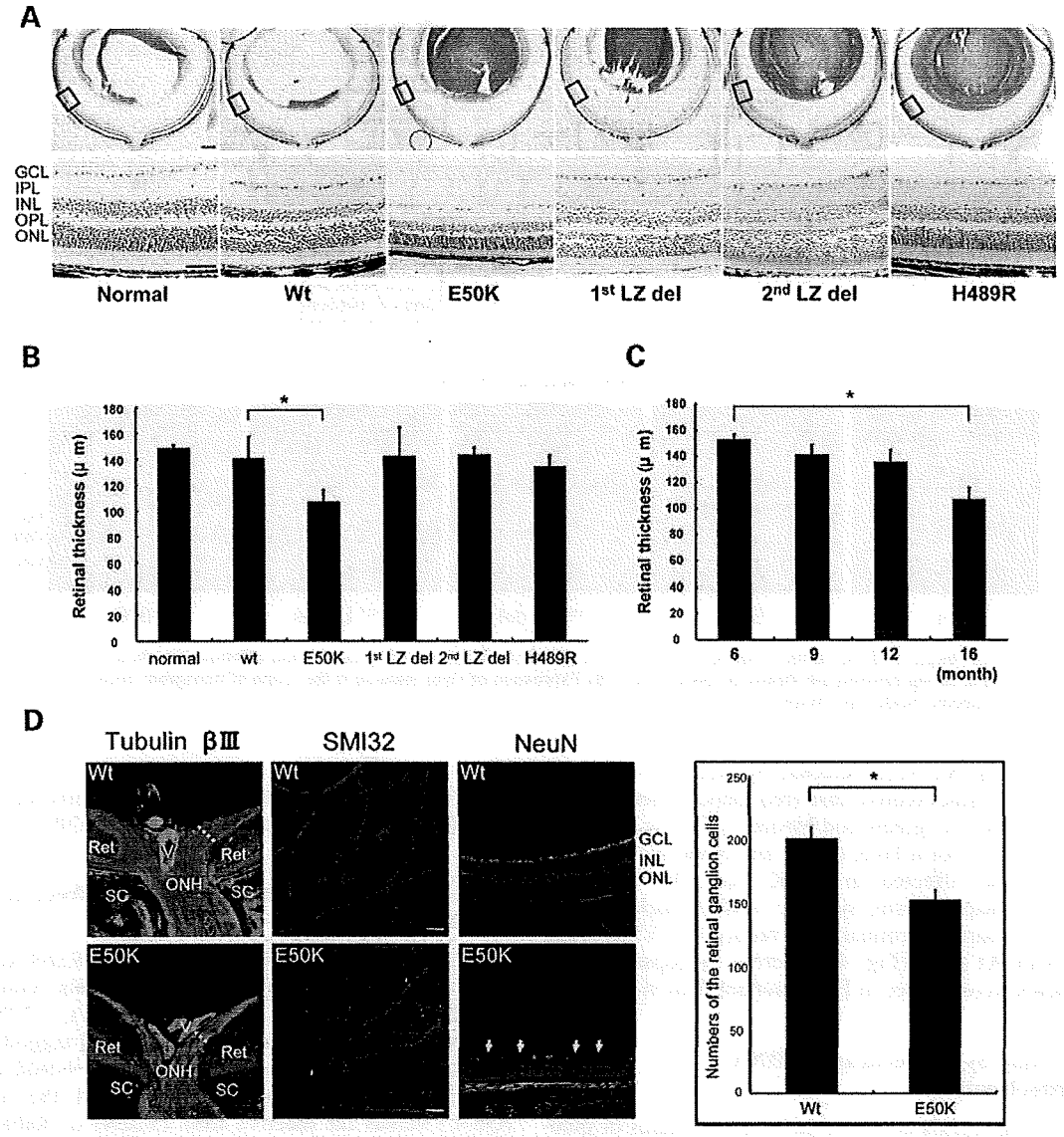

Figure 2. Comparison of retina morphology of normal, Wt and mutant transgenic mice. (**A**) HE staining of retina sections of 16-month-old normal and transgenic mice. Scale bar: 200 μm (upper panel), 50 μm (lower panel). (**B**) Quantification of the retina thickness measurements of different transgenic lines at 16 months of age. Six retina samples were measured in each group. Significant thinning of the retina was observed only for E50K mice ($^*P < 0.05$). (**C**) Quantification of the retina thickness measurements of E50K mice of different ages (6 to 16 months; $n = 6$ for each time point). E50K mice showed statistically significant retinal thinning at 16 months of age. (**D**) Tubulin β-III immunostaining of the Wt and E50K mice at the optic nerve head (scale bar: 50 μm). Reduction of the RGC number at the peripheral retina is shown by NeuN immunostaining of paraffin section and SMI32 immunostaining of flat mount retina for Wt and E50K mice (scale bar: 100 μm). RGCs were counted over entire paraffin sections for NeuN immunostaining. Right panel represents quantification of these results. Significant loss of the RGCs was observed in the E50K mice compared with Wt ($^*P < 0.05$).

(JOAG) (6,8–11,25–27). E50K, a substitution of glutamic acid by lysine at amino acid 50, is exclusively associated with the familial and sporadic forms of NTG (6,8,11), and that phenotype is, on an average, more severe compared with NTG without the E50K mutation (Supplementary Material) (6). A study by Hauser *et al.* (12) also reported a more severe glaucomatous phenotype in a patient with E50K mutation than that in the other NTG patient. The H486R mutation is reportedly associated with both NTG and JOAG (4,26). Histidine 486 is an evolutionarily conserved residue located at the C-terminus, where five other proteins, adenovirus E3-14.K, huntingtin, metabotrophic glutamate receptor 1-a, myosin VI, ring finger protein 11, can interact with Optn (Fig. 1A). On the other hand, we chose 1st and 2nd LZ del as the transgenic construct design. As shown in Figure 1A, both LZ regions are binding sites for various functional molecules—1st LZ: Rab8 and FOS; 2nd LZ: Huntingtin, E3-14.7K, Myosin6, mGluR1, RNF11. To elucidate the functional defect which may occur by deleting these regions, we generated 1st and 2nd LZ del transgenic mice.

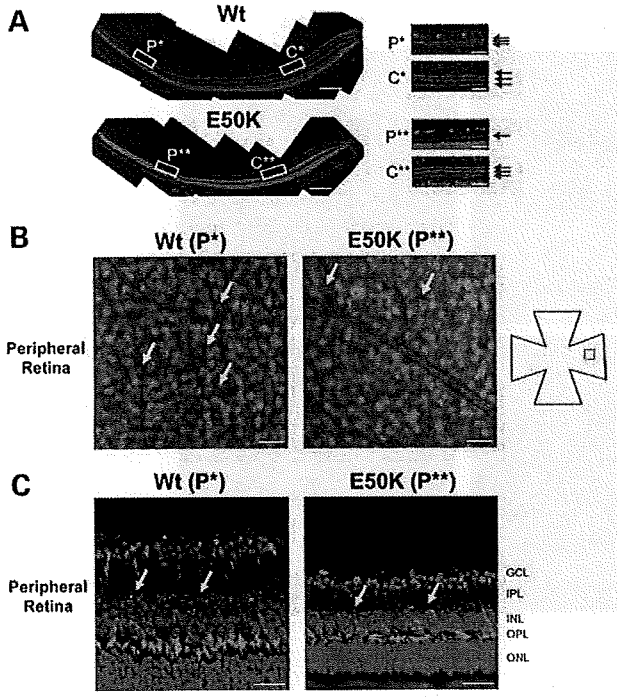

Figure 3. Changes in the retina of E50K mice. (**A**) Immunostaining of the retina sections with anti-calretinin antibody, a specific marker for RGCs and amacrine cells. Disruption of synapses between RGCs and amacrine cells was observed in the peripheral retina of E50K but not control mice (yellow box, P**). Scale bar: 20 μm. (**B**) Immunostaining of the flat mount retina with ChAT (red) and NeuN (green). A significant number of starburst amacrine cells were lost in the RGC layer in the peripheral retina of E50K mutant mice (P**) compared with Wt mice (P*). Scale bar: 50 μm. (**C**) Immunostaining of the retina sections with tyrosine hydroxylase (red) and PKC α (green), specific markers for dopaminergic amacrine cells and rod bipolar cells, respectively. Amacrine cell loss and size reduction of bipolar cells were observed. Scale bar: 20 μm.

Taken together, we hypothesized that each OPTN transgenic line would show distinct phenotype because of different locations of mutations, influencing different OPTN-interacting proteins. Surprisingly, only E50K mutant showed severe histopathological changes in mice. The E50K mice showed not only loss of RGCs, but also progressive retinal degeneration exclusively in the peripheral region (Figs. 2–4). Immunolabeling of ssDNA demonstrated that apoptotic changes occurred in all retinal cell layers. The number of cells in different retinal layers, including amacrine, bipolar and photoreceptor cells, and thickness of all retinal cell layers were reduced in the peripheral retina of E50K mice.

Herein, a question may rise from these findings in E50K mice: why is neuronal degeneration eminent at the peripheral retina, not at the central retina? Previous reports have indicated that mouse models of glaucoma follow similar natural courses of peripheral retinal degeneration. These include the well-known glaucoma mouse model, the DBA/2J mouse, and recently reported GLAST-deficient mouse, where all layers of the peripheral retina were shown to be affected, leading to a significant reduction of retinal thickness (24,28). The myocilin Tyr437His transgenic mouse, a POAG mouse model, also develops RGC loss at the peripheral retina and retinal degeneration (29,30). These three mouse models all share a pattern of peripheral degeneration with Optn E50K mice. In general, glaucoma most often affects peripheral visual field at early stages of the disease, whereas deterioration of the central retina can be seen only at later stages of the disease (31). We can speculate that the increased sensitivity of peripheral RGCs is associated with longer non-myelinated axons compared with the central RGCs, but this would not explain the degeneration of other neuronal cells. Further investigation is required to explain the difference of E50K susceptibility between mouse and human at the peripheral retina. The fact that E50K mice develop a phenotype of peripheral RGC degeneration which is similar to the previous glaucoma mouse models suggests that later stages of cellular and molecular mechanisms for neuronal degeneration are shared between NTG and POAG. Therefore, the use of E50K mice in exploring the mechanisms of NTG pathogenesis, as well as the development of new therapeutic interventions, holds great promise.

Rab8 belongs to a family of small GTP-binding proteins which act as regulators of multiple cellular processes. Rab GTPases regulate all stages of membrane trafficking, including vesicle transport, cargo sorting, transport, tethering and fusion (32). Rab8 has been shown to be involved in polarized membrane transport and regulation of vesicular transport from the trans-Golgi network (33). Recently, OPTN was demonstrated to protect survival of NIH3T3 cells under oxidative stress by relocating to the nucleus in an Rab8-dependent manner, whereas E50K lost the ability to translocate to the nucleus (34). These previous functional analyses of the protein–protein interaction reveal that OPTN–Rab8 complex is involved in multiple functions that are essential for retinal and optic nerve health. Thus, alterations of this complex by E50K mutation may influence the entire cellular function, leading to glaucomatous-like pathology.

Our study demonstrated for the first time a direct protein–protein interaction of OPTN and Rab8 at the Golgi-complex and spreading vesicles (Fig. 6C), which was completely abolished by E50K mutation. The downstream effect of this disruption can be predicted by two studies by Buss and colleagues and Canals and colleagues, who demonstrated the importance of OPTN–Rab8 complex with myosin VI or huntingtin for post-Golgi trafficking, respectively (18,35). Sahlendaer *et al.* (18) demonstrated that OPTN and active Rab8 interact with myosin VI and this is essential for the formation of Golgi ribbon and exocytosis. del Toro *et al.* (35) demonstrated that a mutation in huntingtin reduces interaction with OPTN–Rab8 complex, resulting in delocalization of the complex in Golgi and impairment of post-Golgi trafficking. In both studies, OPTN–Rab8 was considered essential component of post-Golgi trafficking system, whereas OPTN served as an effecter protein of Rab8 and a binding partner of the actin-based motor protein myosin VI. Disruption of this complex may result in a significant reduction of selected protein transport within the cell and to the cell surface for secretion. It would be interesting to investigate what type of cargo is affected by the E50K mutation and if cells be rescued by supplementing this cargo molecule. If these proteins can be

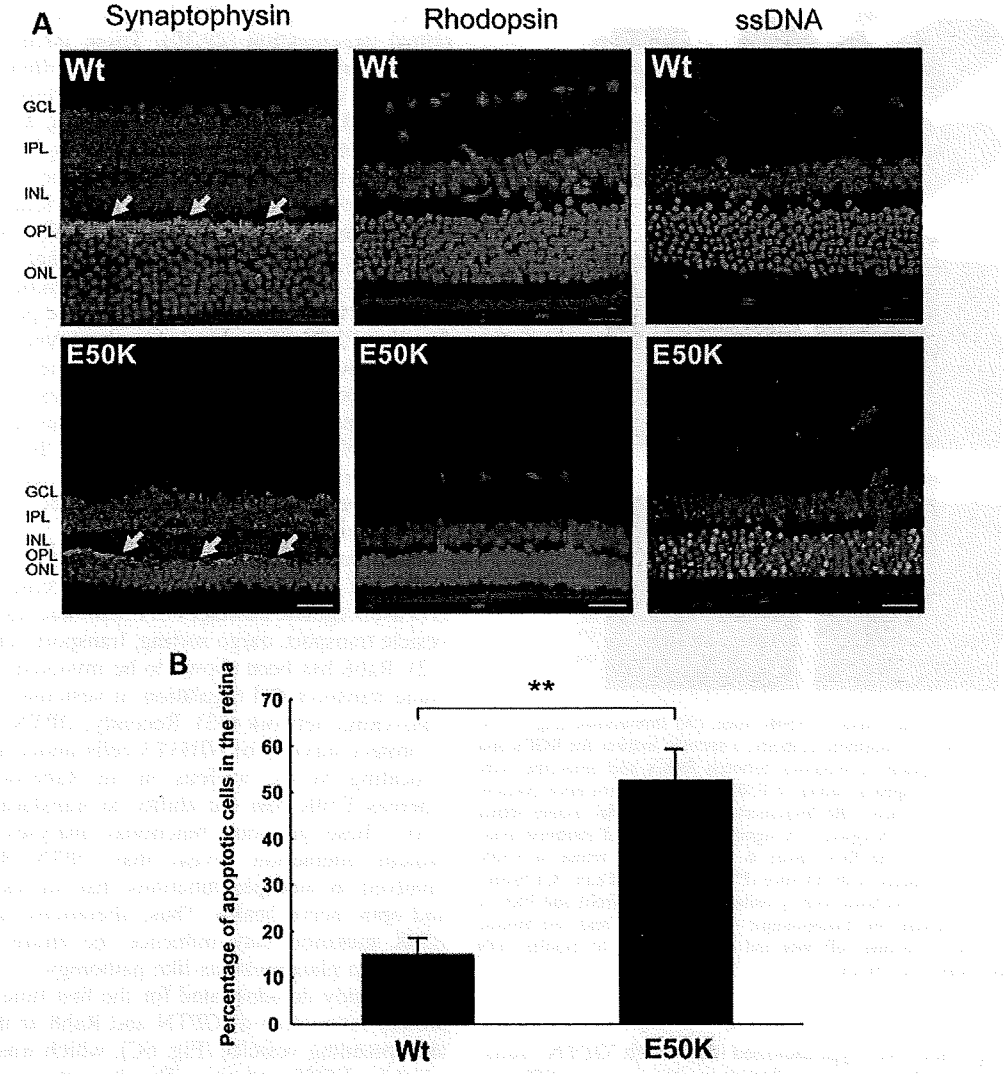

Figure 4. Degeneration of the OPL and ONL in the peripheral retina of E50K mice. **(A)** Immunostaining of the retina sections with synaptophysin, rhodopsin and ssDNA, specific markers for neuronal presynaptic vesicles, rod photoreceptors and apoptosis cells, respectively. Synapse disruption (arrow), rod photoreceptor cells degeneration and apoptosis cells were observed in the OPL and/or ONL in the peripheral retina of E50K mice. Scale bar: 20 μm. **(B)** Percentage of apoptotic cells in the ONL ($n = 6$, $^{**}P < 0.01$).

identified, it may serve as potential therapeutic approach to treat glaucoma patients with E50K mutation.

In the photoreceptor, Rab8 has a pivotal role of docking and fusion in rhodopsin trafficking (36) and cooperating with Bardet–Biedl syndrome proteins in ciliary membrane biogenesis (37,38). One possible explanation about the significant apoptotic changes in the ONL suggests that disruption of OPTN–Rab8 complex may affect the trafficking not only in the RGCs but also in the photoreceptors. Until now, there are no reports about the correlation between OPTN and Rab8 in the photoreceptors, or OPTN-mutated glaucoma and photoreceptor function. Considering trafficking malfunction via OPTN mutation as the etiology of glaucoma, E50K mice provides a good animal model to explore the pathogenesis of RGC and photoreceptor.

MATERIALS AND METHODS

Cloning of mouse Optn and site-directed mutagenesis

Total RNA was extracted from a fresh C57BL/6N mouse brain tissue using TRIzol (Invitrogen, Carlsbad, CA, USA) and reverse-transcribed into first-strand cDNA using oligo-dT adaptor primer and SuperScript First-Strand Synthesis System for RT–PCR (Invitrogen). OPTN cDNA was amplified by PCR using oligonucleotides 5′-cggaattccgatgtcccatcaacctctgag-3′ and 5′-cggaattccgtcaaatgatgcagtccatca-3′ as primers. The amplified DNA fragment was purified using a MinElute gel extraction kit (Qiagen, Hilden, Germany), ligated into pBluescript II (KS-) (Agilent Technologies, Santa Clara, CA, USA) and sequenced using the M13 primers and ABI PRISM 3130 (Applied Biosystems, Foster City, CA, USA). Site-directed

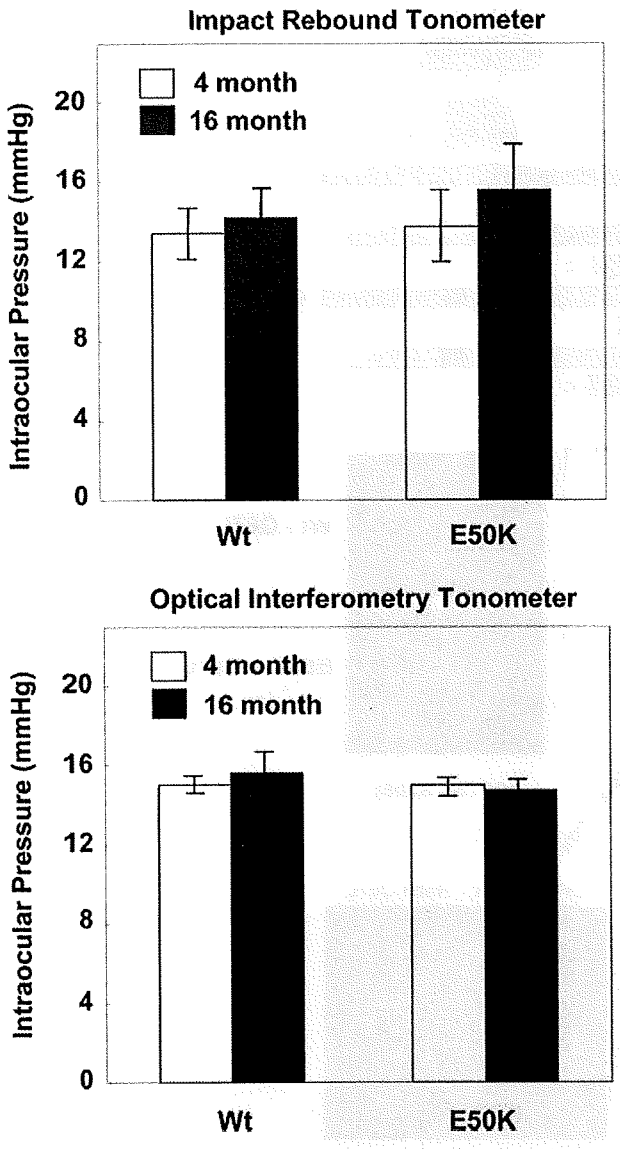

Figure 5. IOP measurement of Wt and E50K mice. IOP was measured using an impact-rebound tonometer and an optical interferometry tonometer between 9 AM and noon in 4-month and 16-month-old mice. Both methods gave similar results (IOP of 15 ± 1 mmHg) for Wt and transgenic mice at both ages examined ($n = 6$).

mutagenesis was carried out to produce cDNA corresponding to the deletion of the E50K mutation, the first leucine zipper (1st LZ del), deletion of the second leucine zipper (2nd LZ del) and the H489R mutation. The following primers were used: 5′-cagctcaaactcaactccgg-3′ and 5′-atgctccacttcctgctcca-3′ for 1st LZ del, 5′-aaatgaaggaactcctggttaagaaccaccagctgaaagaa-3′ and 5′-ttctttcagctggtggttcttaaccaggagttccttcattt-3′ for E50K, 5′-gagaccatggccgtcctc-3′ and 5′-caacatcttgtccacctttctg-3′ for 2nd LZ del and 5′-gcagcaagagagaagattcgtgaagaaaaggagcagc-3′ and 5′-gctgctccttttcttcacgaatcttctctcttgctgc-3′ for H489R. Plasmids were digested with *Eco*RI, purified by agarose gel electrophoresis and recovered using the MinElute gel extraction kit according to the manufacturer's protocol. The cDNA inserts were ligated into *Eco*RI-digested pCMVHA vector (Takara Bio USA, Madison, WI, USA). HA-tagged Optns were amplified by PCR using oligonucleotides 5′-ccgctcgagcgccaccatgatg tacccatacgatgttcc-3′ and 5′-ccgctcgagcggtcaaatgatgcagtccatca-3′ as primers. HA-tag was inserted at the N-terminus of Optn constructs for the detection of proteins expressed by the transgene. The amplified DNA fragments were purified using a MinElute gel extraction kit (Qiagen), ligated into the expression vector and sequenced as described earlier.

Development of transgenic mice overexpressing mutant Optn

The expression vector pCAGGS containing chicken beta-actin promoter with CMV enhancer kindly provided by Dr Junichi Miyazaki of Osaka University was used for strong ubiquitous expression of the transgene in mice. cDNA inserts were released from the pCAGGS vector using *Sal*I and *Bam*HI. These restriction fragments were injected into pronuclear-stage BDF1/C57BL6N embryos, and transgenic mice were generated at PhoenixBio Co., Ltd (Tochigi, Japan). Offspring were screened for the transgene by isolating genomic DNA from tail biopsies followed by PCR. Primers used for PCR were 5′-ctctagagcctctgctaaccatgt-3′ and 5′-ccatggccataagagcg taa-3′. To determine copy number of transgenes, real-time PCR was performed using TaqMan MGB probe (Applied Biosystems), according to manufacturer's standard protocols. Primers and probe for the mouse beta-actin were 5′-AGGC CAACCGTGAAAAGATG-3′ (forward), 5′-TGAGAAGCTG GCCAAAGAGAA-3′ (reverse) and 5′-CCCAGGTCAGTAT CC-3′ (probe); for the CAG promoter were 5′-CCGCAGCC ATTGCCTTT-3′ (forward), 5′-TTCGGCTCCGCACAGATT-3′ (reverse) and 5′-CGCAGGGACTTCC-3′ (probe). To determine the absolute amount of the copy number of beta-actin, PCR products of mouse beta-actin amplified from genomic DNA were cloned into the pCAGGS vector. The copy number of beta-actin gene in mouse genome was measured with real-time PCR analyses, the purified plasmid DNAs were used as standards. To determine the transgene copy number, multiplex quantitative PCR was performed for both CAG promoter as a target and beta-actin gene as a reference. All experiments with mice were performed in accordance with the Association for Research in Vision and Ophthalmology Statement for the Use of Animals in Vision Research.

Histology and immunohistochemistry

Mice were sacrificed with Nembutal (150 mg/kg) i.p., and the eyes were removed quickly. For histology, mouse eyes were dissected and immersed in Davidson's solution fixative overnight at 4°C. The eyes were embedded in paraffin and sectioned at 5 μm thickness along the vertical meridian through the optic nerve head. After deparaffinization and rehydration, sections were stained with hematoxylin and eosin (HE) staining. Images of HE staining were collected with Nikon Eclipse light microscope (Nikon, Tokyo, Japan).

For immunohistochemistry, after deparaffinization and rehydration, eye sections were treated with Target Retrieval Solution (DakoCytomation, Denmark). These sections were incubated

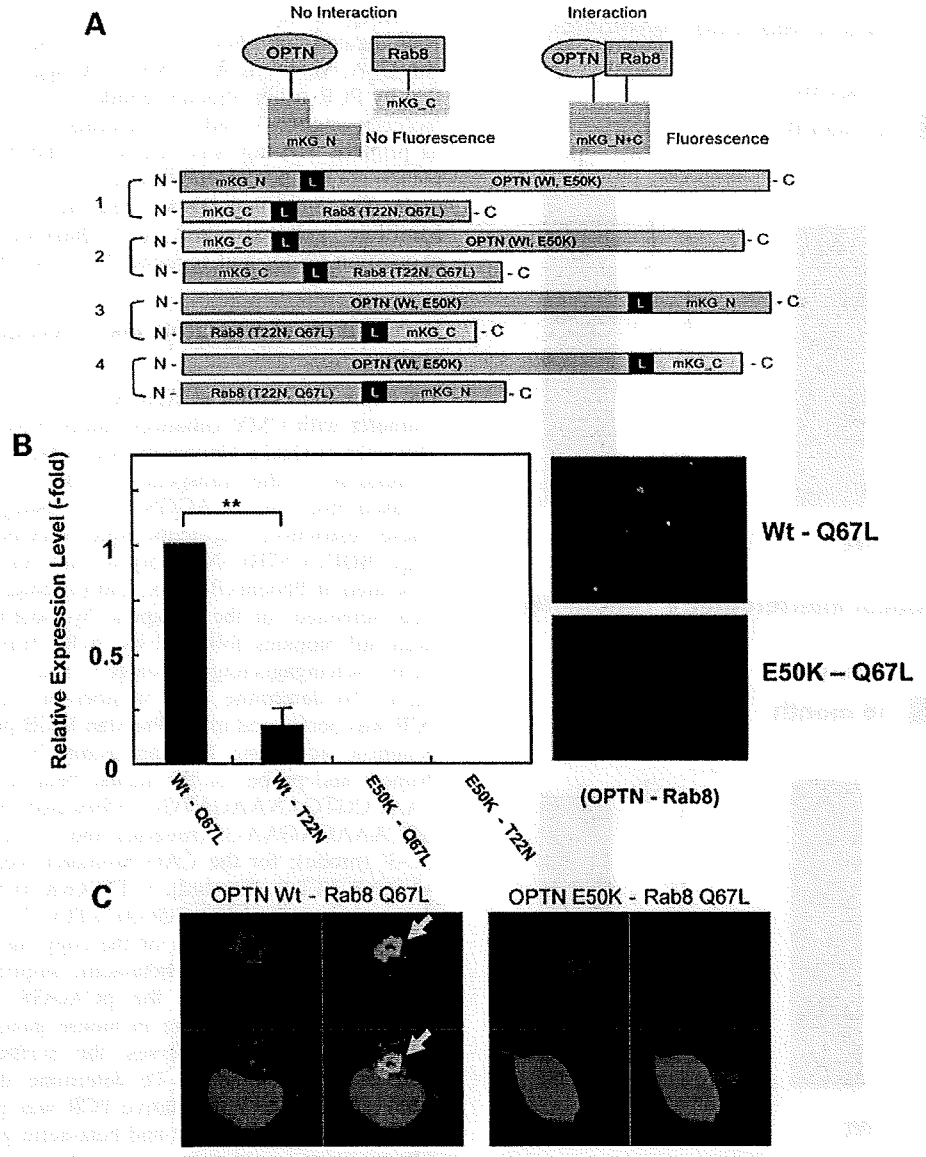

Figure 6. Disruption of OPTN–Rab8 interaction by the E50K mutation. (**A**) A diagram of cDNA constructs used in experiments to study protein–protein interaction. (**B**) The protein–protein interaction of OPTN Wt and E50K with Rab8 T22N (GDP inactive form), and Q67L (GTP active form) was measured in RGC-5 cells as described in Materials and Methods. Interaction of OPTN Wt and Q67L-active form of Rab8 was increased five times over Rab8 T22N-inactive form of Rab8 protein (**$P < 0.01$). E50K did not show any interaction with any construct including the active form of Rab8 ($n = 6$). (**C**) Co-localization of the OPTN–Rab8 complex (green) and Golgi marker GM130 (red). COS1 cells were transfected with constructs encoding indicated constructs and stained with antibodies against GM130 48 h after transfection as described in Materials and Methods. Nuclei (blue) were stained with DAPI.

with blocking solution for 1 h followed by overnight incubation with primary antibody against HA tag (1:500 dilution; Sigma-Aldrich, St Louis, MO, USA), OPTN (1:500 dilution; kind gift from Dr Mansoor Sarfarazi, University of Connecticut), tubulin β-III isoform (1:100 dilution; Millipore, Billerica, MA, USA), NeuN (1:100 dilution; Millipore), calretinin (1:500 dilution; Sigma), tyrosine hydroxylase (1:100 dilution; Millipore), PKC α (1:500 dilution; Millipore), rhodopsin (1:200 dilution; Santa Cruz, CA, USA), synaptophysin (1:500 dilution; Abcam, Cambridge, MA, USA) or ssDNA (1:500 dilution; Immuno-Biological Laboratories, Gunma, Japan) in phosphate-buffered saline (PBS) containing 1% BSA at 4°C. Slides were washed in PBS and then incubated with Alexa 488 or Alexa 568 (1:500 dilution; Invitrogen)-conjugated anti-mouse or rabbit IgG and 4′,6′-diamidino-2-phenylindole (DAPI) for nuclear staining for 1 h at room temperature. The stained tissues were examined using confocal fluorescence laser microscope (Radiance 2000, Bio-Rad Laboratories, Hercules, CA, USA). Control slides were processed similarly, except for the omission of primary antibodies (data not shown).

Whole-mount immunostaining

The whole-mount immunostaining was performed essentially as described (39,40). Briefly, neural retinas were separated from the posterior eyes, fixed in 4% PFA/PBS for 2 h on ice and incubated with the anti-SMI32 (1:200 dilution; Sternberger Monoclonals, Baltimore, MD, USA), anti-ChAT (1:100 dilution; Millipore) or anti-active NeuN (1:250 dilution; Millipore) antibody for 7 days at 4°C. Slides were washed in PBS containing 0.1% Triton X-100 and then incubated with Alexa 488 or Alexa 568 (1:500 dilution; Invitrogen)-conjugated anti-mouse or rabbit IgG/DAPI for 2 days at 4°C. Whole-mounted retinal samples were placed on slides, with the vitreous facing up. Radial cuts were made in the peripheral retina, and the retinal tissue was flattened with a fine brush. The retinas were then mounted with Vectashield (Vector Laboratories, Burlingame, CA, USA) and evaluated with a confocal microscope.

Measurement of IOP

The average IOP for each genotype was recorded. IOP was measured using an impact-rebound tonometer (Colonal Medical Supply, Franconia, NH, USA) and optical interferometry tonometer (FISO Technologies, Quebec, Canada) for mice of each genotype as described (29). Using the rebound tonometer, we were able to measure IOP in awake and non-sedated mice of various ages, whereas optical interferometry tonometry was performed on anesthetized animals. Measurement of IOP was always performed in the morning between 10 and 12 AM. The mice successfully assessed for each genotype and age were 18 weeks and 16 months.

Measurement of OPTN–Rab8 interaction

OPTN–Rab8 interaction analysis was performed using Coral-Hue® Fluo-chase Kit (MBL, Tokyo, Japan). Based on the instruction manual, we constructed OPTN Wt, E50K, Rab8 Q67L (GTP-bound active form), Rab8 T22N (GDP-bound inactive form), with fluorescence tag protein (mKG_N or mKG_C) on either N-terminal or C-terminal (Fig. 6A). RGC-5 and COS1 cells were transfected by each pair of the plasmid mixtures using Fugene HD (Roche Diagnostics, Mannheim, Germany). Forty-eight hours after transfection, the medium was replaced to PBS and the cells were observed with inverted microscope (Eclipse TE300, Nikon). To observe localization of OPTN–Rab8 complex, cells were fixed 48 h after transfection with 4% paraformaldehyde in PBS on ice for 20 min. Cells were incubated in blocking buffer (3% bovine serum albumin, 0.1% Triton X-100 in PBS) and then with anti-GM130 antibody (BD Bioscience, San Jose, CA, USA) at room temperature for 1 h each. Cells were washed three times with PBS-T (0.1% Triton X-100 in PBS) and incubated with Alexa-568-conjugated secondary antibody for 1 h at room temperature. Slides were washed, mounted and analyzed by confocal microscopy.

Statistical analysis

All data were expressed as the mean ± standard deviation. Statistical differences were analyzed by the ANOVA or Student's *t*-test. $^*P < 0.05$ was considered statistically significant.

SUPPLEMENTARY MATERIAL

Supplementary Material is available at *HMG* online.

ACKNOWLEDGEMENTS

The authors thank T.V. Johnson, S. Zigler, Jr, for critical reading of the manuscript and K. Fujinami for helpful comments.

Conflict of Interest statement. None declared.

FUNDING

This research was supported in part by the grants to T.I. by the Japan Ministry of Health, Labor, and Welfare, to T.I. and M.A. by the Japan Ministry of Education, Culture, Sports, Science and Technology and to T.I. for Japan Society for the Promotion Science Fellowship for Z.C. Funding to pay the Open Access publication charges for this article was provided by the Japan Ministry of Health, Labor, and Welfare.

REFERENCES

1. Quigley, H.A. (1996) Number of people with glaucoma worldwide. *Br. J. Ophthalmol.*, **80**, 389–393.
2. Quigley, H.A. and Broman, A.T. (2006) The number of people with glaucoma world wide in 2010 and 2020. *Br. J. Ophthalmol.*, **90**, 262–267.
3. Iwase, A., Suzuki, Y., Araie, M., Yamamoto, T., Abe, H., Shirato, S., Kuwayama, Y., Mishima, H.K., Shimizu, H., Tomita, G. *et al.* (2004) The prevalence of primary open-angle glaucoma in Japanese: the Tajimi Study. *Ophthalmology*, **111**, 1641–1648.
4. Stone, E.M., Fingert, J.H., Alward, W.L., Nguyen, T.D., Polansky, J.R., Sunden, S.L., Nishimura, D., Clark, A.F., Nystuen, A., Nichols, B.E. *et al.* (1997) Identification of a gene that causes primary open angle glaucoma. *Science*, **275**, 668–670.
5. Stoilov, I., Akarsu, A.N. and Sarfarazi, M. (1997) Identification of three different truncating mutations in cytochrome P4501B1 (CYP1B1) as the principal cause of primary congenital glaucoma (buphthalmos) in families linked to the GLC3A locus on chromosome 2p21. *Hum. Mol. Genet.*, **6**, 641–647.
6. Rezaie, T., Child, A., Hitchings, R., Brice, G., Miller, L., Coca-Prados, M., Heon, E., Krupin, T., Ritch, R., Kreutzer, D. *et al.* (2002) Adult-onset primary open-angle glaucoma caused by mutations in optineurin. *Science*, **295**, 1077–1079.
7. Monemi, S., Spaeth, G., DaSilva, A., Popinchalk, S., Ilitchev, E., Liebmann, J., Ritch, R., Heon, E., Crick, R.P., Child, A. *et al.* (2005) Identification of a novel adult-onset primary open-angle glaucoma (POAG) gene on 5q22.1. *Hum. Mol. Genet.*, **14**, 725–733.
8. Aung, T., Rezaie, T., Okada, K., Viswanathan, A.C., Child, A.H., Brice, G., Bhattacharya, S.S., Lehmann, O.J., Sarfarazi, M. and Hitchings, R.A. (2005) Clinical features and course of patients with glaucoma with the E50K mutation in the optineurin gene. *Invest. Ophthalmol. Vis. Sci.*, **46**, 2816–2822.
9. Leung, Y.F., Fan, B.J., Lam, D.S., Lee, W.S., Tam, P.O., Chua, J.K., Tham, C.C., Lai, J.S., Fan, D.S. and Pang, C.P. (2003) Different optineurin mutation pattern in primary open-angle glaucoma. *Invest. Ophthalmol. Vis. Sci.*, **44**, 3880–3884.
10. Fuse, N., Takahashi, K., Akiyama, H., Nakazawa, T., Seimiya, M., Kuwahara, S. and Tamai, M. (2004) Molecular genetic analysis of optineurin gene for primary open-angle and normal tension glaucoma in the Japanese population. *J. Glaucoma*, **13**, 299–303.
11. Alward, W.L., Kwon, Y.H., Kawase, K., Craig, J.E., Hayreh, S.S., Johnson, A.T., Khanna, C.L., Yamamoto, T., Mackey, D.A., Roos, B.R. *et al.* (2003) Evaluation of optineurin sequence variations in 1,048 patients with open-angle glaucoma. *Am. J. Ophthalmol.*, **136**, 904–910.

12. Hauser, M.A., Sena, D.F., Flor, J., Walter, J., Auguste, J., Larocque-Abramson, K., Graham, F., Delbono, E., Haines, J.L., Pericak-Vance, M.A. *et al.* (2006) Distribution of optineurin sequence variations in an ethnically diverse population of low-tension glaucoma patients from the United States. *J. Glaucoma*, **15**, 358–363.
13. Chalasani, M.L., Radha, V., Gupta, V., Agarwal, N., Balasubramanian, D. and Swarup, G. (2007) A glaucoma-associated mutant of optineurin selectively induces death of retinal ganglion cells which is inhibited by antioxidants. *Invest. Ophthal. Vis. Sci.*, **48**, 1607–1614.
14. Faber, P.W., Barnes, G.T., Srinidhi, J., Chen, J., Gusella, J.F. and MacDonald, M.E. (1998) Huntingtin interacts with a family of WW domain proteins. *Hum. Mol. Genet.*, **7**, 1463–1474.
15. Moreland, R.J., Dresser, M.E., Rodgers, J.S., Roe, B.A., Conaway, J.W., Conaway, R.C. and Hanas, J.S. (2000) Identification of a transcription factor IIIA-interacting protein. *Nucleic Acids Res.*, **28**, 1986–1993.
16. Hattula, K. and Peranen, J. (2000) FIP-2, a coiled-coil protein, links Huntingtin to Rab8 and modulates cellular morphogenesis. *Curr. Biol.*, **10**, 1603–1606.
17. Park, B.C., Shen, X., Samaraweera, M. and Yue, B.Y. (2006) Studies of optineurin, a glaucoma gene: Golgi fragmentation and cell death from overexpression of wild-type and mutant optineurin in two ocular cell types. *Am. J. Pathol.*, **169**, 1976–1989.
18. Sahlender, D.A., Roberts, R.C., Arden, S.D., Spudich, G., Taylor, M.J., Luzio, J.P., Kendrick-Jones, J. and Buss, F. (2005) Optineurin links myosin VI to the Golgi complex and is involved in Golgi organization and exocytosis. *J. Cell. Biol.*, **169**, 285–295.
19. Miyamoto-Sato, E., Ishizaka, M., Horisawa, K., Tateyama, S., Takashima, H., Fuse, S., Sue, K., Hirai, N., Masuoka, K. and Yanagawa, H. (2005) Cell-free cotranslation and selection using *in vitro* virus for high-throughput analysis of protein–protein interactions and complexes. *Genome Res.*, **15**, 710–717.
20. Colland, F., Jacq, X., Trouplin, V., Mousin, C., Groizeleau, C., Hamburger, A., Meil, A., Wojcik, J., Legrain, P. and Gauthier, J.M. (2004) Functional proteomics mapping of a human signaling pathway. *Genome Res.*, **14**, 1324–1332.
21. Anborgh, P.H., Godin, C., Pampillo, M., Dhami, G.K., Dale, L.B., Cregan, S.P., Truant, R. and Ferguson, S.S. (2005) Inhibition of metabotropic glutamate receptor signalling by the huntingtin binding protein optineurin. *J. Biol. Chem.*, **280**, 34840–34848.
22. Sudhakar, C., Nagabhushana, A., Jain, N. and Swarup, G. (2009) NF-kappaB mediates tumor necrosis factor alpha-induced expression of optineurin, a negative regulator of NF-kappaB. *PLoS One*, **4**, e5114.
23. Journo, C., Filipe, J., About, F., Chevalier, S.A., Afonso, P.V., Brady, J.N., Flynn, D., Tangy, F., Israël, A. and Vidalain, P.O. (2009) NRP/optineurin cooperates with TAX1BP1 to potentiate the activation of NF-kappaB by human T-lymphotropic virus type 1 tax protein. *PLoS Pathog.*, **5**, e1000521.
24. Harada, T., Harada, C., Nakamura, K., Quah, H.M., Okumura, A., Namekata, K., Saeki, T., Aihara, M., Yoshida, H., Mitani, A. *et al.* (2007) The potential role of glutamate transporters in the pathogenesis of normal tension glaucoma. *J. Clin. Invest.*, **117**, 1763–1770.
25. Funayama, T., Ishikawa, K., Ohtake, Y., Tanito, T., Kurosaka, D., Kimura, I., Suzuki, K., Ideta, H., Nakamoto, K., Yasuda, N. *et al.* (2004) Variants in optineurin gene and their association with tumor necrosis factor-alpha polymorphisms in Japanese patients with glaucoma. *Invest. Ophthalmol. Vis. Sci.*, **45**, 4359–4367.
26. Weisschuh, N., Neumann, D., Wolf, C., Wissinger, B. and Gramer, E. (2005) Prevalence of myocilin and optineurin sequence variants in German normal tension glaucoma patients. *Mol. Vis.*, **11**, 284–287.
27. Yao, H.Y., Cheng, C.Y., Fan, B.J., Tam, O.S., Tham, C.Y., Wang, D.Y., Lam, S.C. and Pang, C.P. (2006) Polymorphisms of myocilin and optineurin I primary open-angle glaucoma patients. *Zhonghua Yi Xue Za Zhi.*, **86**, 554–559.
28. John, S.W., Smith, R.S., Savinova, O.V., Hawes, N.L., Chang, B., Turnbull, D., Davisson, M., Roderick, T.H. and Heckenlively, J.R. (1998) Essential iris atrophy, pigment dispersion, and glaucoma in DBA/2J mice. *Invest. Ophthalmol. Vis. Sci.*, **39**, 951–962.
29. Senatorov, V., Malyukova, I., Fariss, R., Wawrousek, E.F., Swaminathan, S., Sharan, S.K. and Tomarev, S. (2006) Expression of mutated mouse myocilin induces open-angle glaucoma in transgenic mice. *J. Neurosci.*, **26**, 11903–11914.
30. Zhou, Y., Grinchuk, O. and Tomarev, S.I. (2008) Transgenic mice expressing the Tyr437His mutant of human myocilin protein develop glaucoma. *Invest. Ophthalmol. Vis. Sci.*, **49**, 1932–1939.
31. Foster, P.J., Buhrmann, R., Quigley, H.A. and Johnson, G.J. (2002) The definition and classification of glaucoma in prevalence surveys. *Br. J. Ophthalmol.*, **86**, 238–242.
32. Zerial, M. and McBride, H. (2001) Rab proteins as membrane organizers. *Nat. Rev. Mol. Cell. Biol.*, **2**, 107–117.
33. Huber, L.A., Pimplikar, S., Parton, R.G., Virta, H., Zerial, M. and Simons, K. (1993) Rab8, a small GTPase involved in vesicular traffic between the TGN and the basolateral plasma membrane. *J. Cell. Biol.*, **123**, 35–45.
34. De Marco, N., Buono, M., Troise, F. and Diez-Roux, G. (2006) Optineurin increases cell survival and translocates to the nucleus in a Rab8-dependent manner upon an apoptotic stimulus. *J. Biol. Chem.*, **281**, 16147–16156.
35. del Toro, D., Alberch, J., Lázaro-Diéguez, F., Martín-Ibáñez, R., Xifró, X., Egea, G. and Canals, J.M. (2009) Mutant huntingtin impairs post-Golgi trafficking to lysosomes by delocalizing optineurin/Rab8 complex from the Golgi apparatus. *Mol. Biol. Cell.*, **20**, 1478–1492.
36. Moritz, O.L., Tam, B.M., Hurd, L.L., Peranen, J., Deretic, D. and Papermaster, D.S. (2001) Mutant rab8 impairs docking and fusion of rhodopsin-bearing post-Golgi membranes and causes cell death of transgenic *Xenopus* rods. *Mol. Biol. Cell.*, **12**, 2341–2351.
37. Sato, T., Mushiake, S., Kato, Y., Sato, K., Sato, M., Takeda, N., Ozono, K., Miki, K., Kubo, Y., Tsuji, A. *et al.* (2007) The Rab8 GTPase regulates apical protein localization in intestinal cells. *Nature*, **448**, 366–369.
38. Nachury, M.V., Loktev, A.V., Zhang, Q., Westlake, C.J., Peränen, J., Merdes, A., Slusarski, D.C., Scheller, R.H., Bazan, J.F., Sheffield, V.C. *et al.* (2007) A core complex of BBS proteins cooperates with the GTPase Rab8 to promote ciliary membrane biogenesis. *Cell*, **129**, 1201–1213.
39. Jakobs, T.C., Libby, R.T., Ben, Y., John, S.W. and Masland, R.H. (2005) Retinal ganglion cell degeneration is topological but not cell type specific in DBA/2J mice. *J. Cell Biol.*, **171**, 313–325.
40. Howell, G.R., Libby, R.T., Jakobs, T.C., Smith, R.S., Phalan, F.C., Barter, J.W., Barbay, J.M., Marchant, J.K., Mahesh, N., Porciatti, V. *et al.* (2007) Axons of retinal ganglion cells are insulted in the optic nerve early in DBA/2J glaucoma. *J. Cell Biol.*, **179**, 1523–1537.

シンポジウムII　緑内障治療の基礎と臨床
—とくにプロスタグランジン点眼薬について—

緑内障遺伝子改変動物の基礎

岩　田　　岳

国立病院機構東京医療センター臨床研究センター(感覚器センター)分子細胞生物学研究部

Glaucoma Mouse Models Development by Gene Manipulation

Takeshi Iwata

Division of Molecular & Cellular Biology, National Institute of Sensory Organs, National Hospital Organization Tokyo Medical Center

眼薬理　Vol. 23　No. 1　2009　別刷

眼薬理 23：67～70，2009©

シンポジウムII　緑内障治療の基礎と臨床—とくにプロスタグランジン点眼薬について—

緑内障遺伝子改変動物の基礎

岩　田　　岳

国立病院機構東京医療センター臨床研究センター(感覚器センター)分子細胞生物学研究部

Glaucoma Mouse Models Development by Gene Manipulation

Takeshi Iwata

Division of Molecular & Cellular Biology, National Institute of Sensory Organs, National Hospital Organization Tokyo Medical Center

これまでに家族性の開放隅角緑内障の原因遺伝子としてミオシリン，オプチニュリン，そしてWDR36の3つが発見されている．後者2つの遺伝子はMansoor Sarfaraziらによって報告されたが，その分子機能や緑内障との関係は十分に明らかにされていない．筆者らはオプチニュリンとWDR36について患者で観察された遺伝子変異を導入したトランスジェニックマウスを作製し，その病態を解析した．

In the past decade, three glaucoma genes have been identified：myocilin, optineurin and WDR36. The latter two genes, optineurin and WDR36, were reported by Mansoor Sarfarazi and colleagues. Here, we report the investigation of those two genes.

〔Japanese Journal of Ocular Pharmacology **23**：67～70, 2009〕

Key words：緑内障，オプチニュリン，WDR36．glaucoma, optineurin, WDR36.

はじめに

開放隅角緑内障は遺伝子，習慣，環境などの複数の危険因子によって発症する多因子疾患と考えられており，特に遺伝要因が強く，家族歴のある遺伝性の緑内障については大型の家系を用いた連鎖解析や相関解析によって，この10年間に3つの遺伝子が発見されている．開放隅角緑内障遺伝子第1号として発見されたミオシリンについてはこれまでにタンパク質の機能解析から細胞内での機能解析，線維柱帯での局在，そしてノックアウトマウス，トランスジェニックマウスなどが作製された．しかしながら特異的な抗体の作製やタンパク質の精製がむずかしく，ノックアウトマウスでは異常は発見されず，同一遺伝子変異についてトランスジェニックマウスとノックインマウスの結果が異なるなど，未だ遺伝子変異から緑内障発症までの分子メカニズムについて，詳細には明らかになっていない．筆者等は開放隅角緑内障遺伝子として2番目，3番目に報告されたオプチニュリン[1]とWDR36[2]について緑内障との関係を変異体トランスジェニックマウスの作製によって解析した．これらのマウスはいずれも神経節細胞の萎縮が観察され，隣接する周辺細胞にも影響していることが明らかとなった．これらのマウスモデルは開放隅角緑内障の発症機序の解明に役立つだけでなく，新たな予防・治療薬の開発にも役立つと考えられる．

I　緑内障マウスモデル

マウスモデルは高眼圧ラットモデルの陰で開発が遅れていたが，近年の遺伝子改変技術の目覚しい進歩によって，複数のノックアウトマウスやトランスジェニックマウスが作製され，これまで困難であった*in vivo*での機能解析が可能になった．トランスジェニックマウス，ノックアウトマウス，ノックインマウスなどの作製は高価ではあるが委託して作製できるようになり，研究室ごとに独自に考案したコンストラクトでマウスモデルが作製できるようになった．マウスは他

〔別刷請求先〕岩田　岳：〒152-8902 東京都目黒区東が丘2-5-1　国立病院機構東京医療センター臨床研究センター(感覚器センター)分子細胞生物学研究部

Reprint requests：*Takeshi Iwata, Division of Molecular & Cellular Biology, National Institute of Sensory Organs, National Hospital Organization Tokyo Medical Center, 2-5-1 Higashigaoka, Meguro-ku, Tokyo 152-8902, JAPAN*

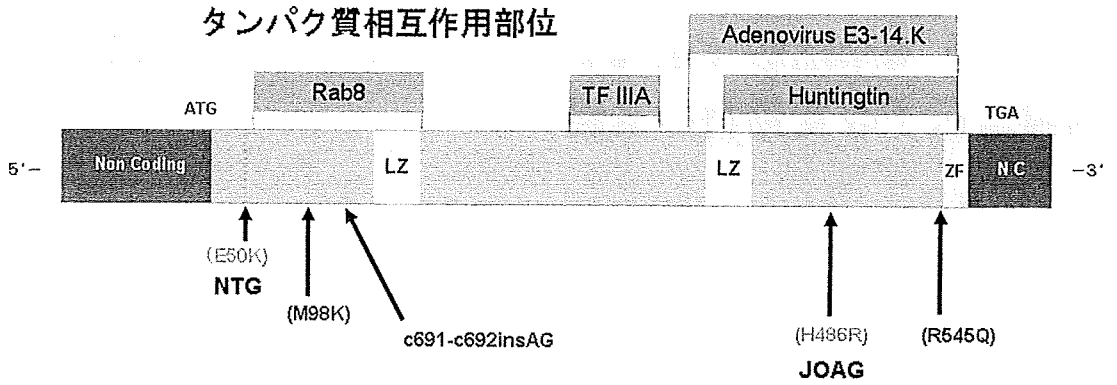

図1　オプチニュリンの cDNA 構造と相互作用タンパク質の位置

・分子量 66 KDa.
・Transcription Factor IIIA, Huntingtin, Rab8, Adenovirus E3-14.7K と相互作用.
・TNF-α によって転写が促進される.

の哺乳類に比べてデータベースが充実しており，遺伝子，タンパク，代謝系，行動パターンに至るまで詳細な情報が入手できる.

遺伝子改変マウスの利点は発症原因が明確なこと，手術による方法に比べて表現型が安定していること，比較的短期間で疾患個体数を増やすことができることである．すでに複数の緑内障マウスが作製されているが，その一つにミオシリンの Tyr437His 変異を発現するトランスジェニックマウスが存在する．このマウスは正常マウスに比べて昼は 2 mmHg，夜は 4 mmHg の眼圧上昇が認められ，生後 1 年目には網膜神経節細胞数の 2 割が減少する．コラーゲンタイプ $1_{\alpha 1}$ サブユニットに遺伝子変異のあるトランスジェニックマウスではコラーゲンのメタロプロテアーゼによる分解が阻害され，生後 9 カ月で眼圧が 4.8 mmHg 上昇することが報告されている．隅角の構造は保持されたまま，網膜神経節細胞層への障害が観察され，開放隅角緑内障マウスモデルとして認識されている.

しかしながらマウスには緑内障モデルとしての欠点も存在する．マウスとヒトでは神経乳頭の構造，視神経乳頭周辺の血管走行，そして発達した篩状板が存在しないなどの違いがある．小さい眼球の取り扱いについても不利な面があり，神経乳頭の鮮明な写真や眼圧測定などで熟練した技術が必要となる.

II　オプチニュリントランスジェニックマウス

筆者らはマウスのオプチニュリン遺伝子をクローニングし，E50K，H486R，第 1 ロイシンジッパー欠損，第 2 ロイシンジッパー欠損のそれぞれの遺伝子変異を導入して，トランスジェニックマウスを作製した．すべての系について約 1 年半にわたって観察を行った結果，E50K 系のみで網膜の異常が観察された．特に周辺網膜における神経節細胞とアストロサイトの萎縮が観察された．疾患マウスの眼圧変化は観察されなかった．オプチニュリンはこれまでに複数のタンパク質と相互作用することが報告されている[3,4]．E50K 変異が Rab8 結合部位に隣接していることから，水晶発振子，免疫沈降法，蛍光タンパク相互作用などの実験手法を用いて OPTN-Rab8 の蛋白相互作用を分析した．Rab8 は GTP に結合した活性型と GDP の非活性型の状態で存在するが，E50K 変異体はいずれの型でも Rab8 との相互作用は認められなかった．Rab8 は Golgi 体から細胞膜への小胞顆粒の輸送に関係するタンパク質の一つであり，オプチニュリンがこの分泌機能に関係している可能性は高い．E50K は全ての分泌機能に影響するのか，あるいは選択的なのか，分泌物は何か，これらの疑問が将来解明されれば，オプチニュリンによ

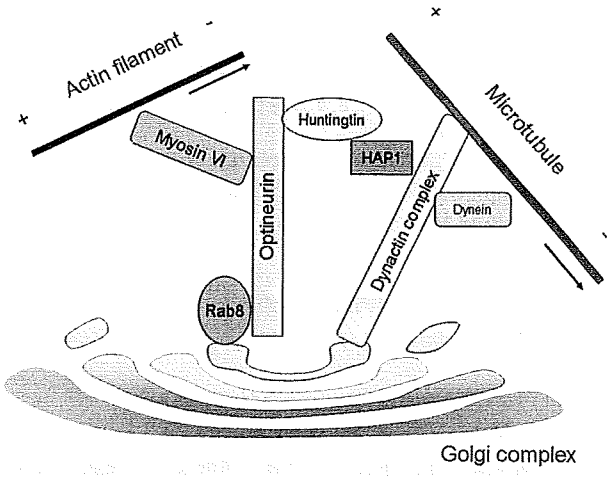

図2　オプチニュリンと相互作用するタンパク質

Golgi 体上で Rab8 とオプチニュリンが小胞顆粒を形成し，ミオシン VI モーターを用いてアクチンフィラメント上を滑走すると予測されている.
(Sahlender DA et al：J Cell Biol 169：285-295, 2005 より)

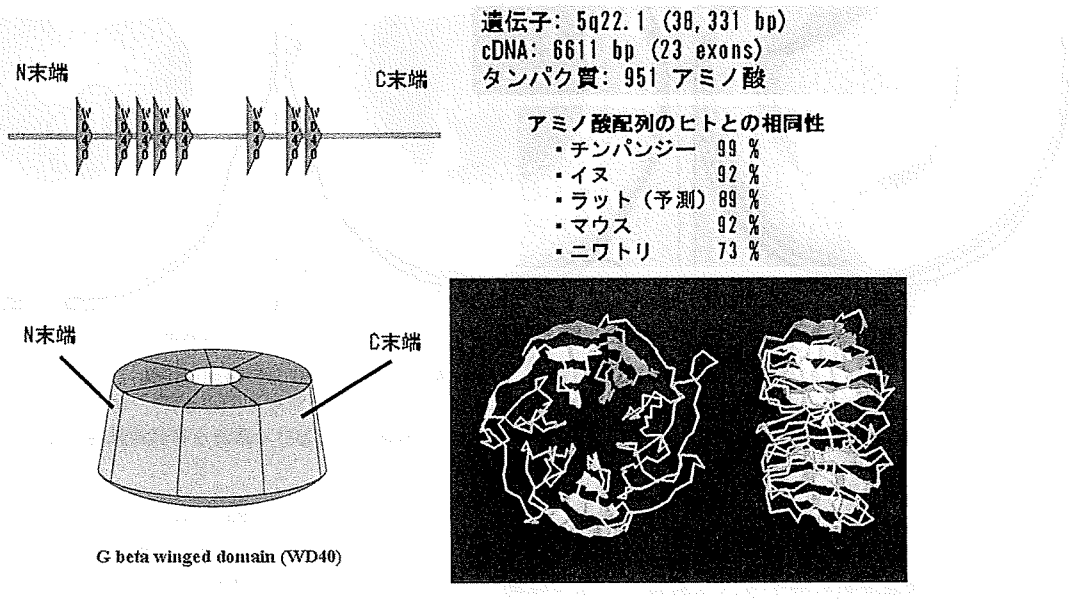

図 3　WDR36 のタンパク質構造

8つの WD40 ドメインから構成される．3つの遺伝子変異は8つ目のドメインにそれぞれ導入され，トランスジェニックマウスが作製された．

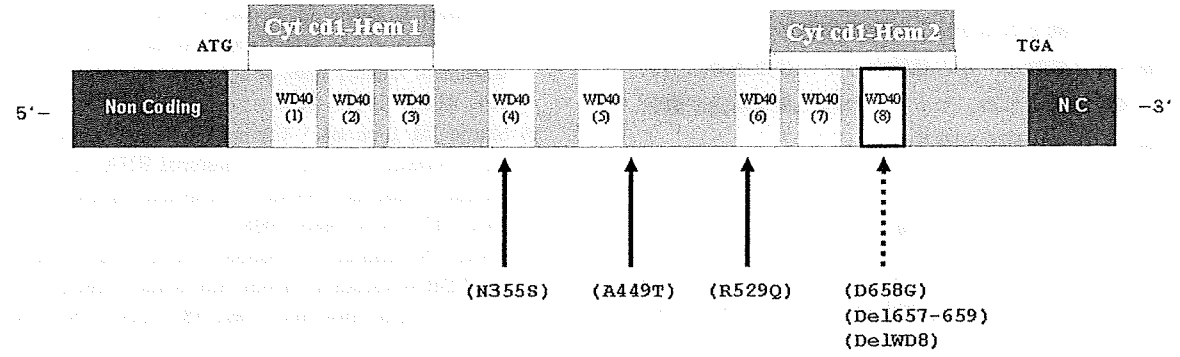

図 4　WDR36 の cCDNA 構造［文献 2）より］

WDR36cDNA と WD40 ドメインの位置．トランスジェニックマウスが作製された3つの遺伝子変異の位置が示されている（点線矢印）．

・タンパク質 105 KDa（951 アミノ酸）．

・Cytochrome cd1-nitrite reductase-like ドメイン．

る緑内障患者に対しての予防・治療法の開発が期待できる．

III　WDR36 トランスジェニックマウス

オプチニュリンの次に作製されたのが WDR36 のトランスジェニックマウスである．WDR36 は約 40 種類のアミノ酸から構成されるドメインを 7〜9 つ束ねた樽構造を形成しており，各ドメインはプロペラの一翼となっている．多数存在する WD タンパク質ファミリーは細胞周期，アポトーシス，転写などの細胞の重要な機能に関係している．WDR36 のアミノ酸配列は動物種間で保存されており，リボゾーム RNA の合成に関与しているとの報告がある[5,6]．トランスジェニックマウスはヒトの D658G，アミノ酸 657-659 の欠損，WD8 の欠損に相当するマウス変異体および，正常体をそれぞれ強制発現して作製された．これらのマウスはオプチニュリンよりも短期間に網膜神経線維の萎縮が発生し，神経節細胞死が観察されたがアストロサイトへの影響は観察されていない．抗 WDR36 抗体を作製し，眼球内での局在を調べた結果，網膜神経節細胞層や内顆粒層，網膜色素上皮細胞に多く発現しており，毛様体上皮にも発現が観察されている．オプチニュリンと同様に眼圧は全てのマウスにおいて正常であった．

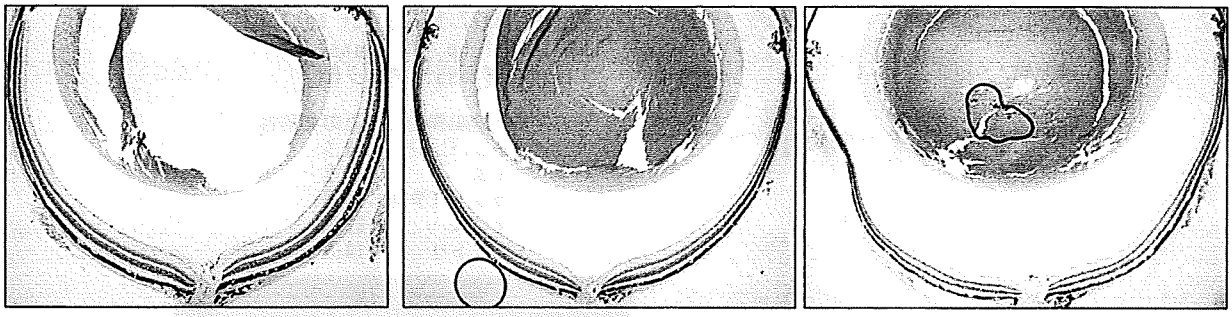

コントロールマウス　　オプチニュリントランスジェニックマウス　　WDR36 トランスジェニックマウス

図 5　OPTN および WDR36 トランスジェニックマウスの眼球切片像

左よりコントロールマウス (16 カ月)，オプチニュリン E50K トランスジェニックマウス (16 カ月)，WDR36 3 アミノ欠損トランスジェニックマウス (6 カ月) の眼球切片．いずれのマウスについても網膜周辺における顕著な神経節線維の萎縮が観察された．

おわりに

今回の作製されたトランスジェニックマウスはオプチニュリンと WDR36 の機能解析には不可欠な動物モデルではあるが，マウスの神経乳頭の構造や血管走行はヒトと異なっており，その病理学的解釈がむずかしい．今後新たな緑内障原因遺伝子や感受性遺伝子が発見され，これらの機能解析のために遺伝子改変技術を用いたマウス，ラット，ウサギモデルが作製されると予測されるが，これらの動物について，これまでに作製された動物モデルの経験からその評価基準について学会での検討が望まれる．ヒトときわめて眼球構造が類似する霊長類モデルへの移行が望まれる．

文　献

1) Rezaie T, Child A, Hitchings R et al : Adult-onset primary open-angle glaucoma caused by mutations in optineurin. *Science* **295** : 1077-1079, 2002
2) Monemi S, Spaeth G, Da Silva A et al : Identification of a novel adult-onset primary open-angle glaucoma (POAG) gene on 5q22.1. *Hum Mol Genet* **14** : 725-733, 2005
3) Obazawa M, Mashima Y, Sanuki N et al : Analysis of porcine optineurin and myocilin expression in trabecular meshwork cells and astrocytes from optic nerve head. *Invest Ophthalmol Vis Sci* **45** : 2652-2659, 2004
4) De Marco N, Buono M, Troise F et al : Optineurin increases cell survival and translocates to the nucleus in a Rab8-dependent manner upon an apoptotic stimulus. *J Biol Chem* **281** : 16147-16156, 2006
5) Skarie JM, Link BA : The primary open-angle glaucoma gene WDR36 functions in ribosomal RNA processing and interacts with the p53 stress-response pathway. *Hum Mol Genet* **17** : 2474-2485, 2008
6) Footz TK, Johnson JL, Dubois S et al : Glaucoma-associated WDR36 variants encode functional defects in a yeast model system. *Hum Mol Genet* **18** : 1276-1287, 2009

*　　*　　*

厚生労働省　創薬基盤推進研究事業

黄斑変性カニクイザルを用いた補体抑制による加齢黄斑変性の予防薬の開発

(H21-政策創薬---般-002)

平成21年度　総括研究報告書

岩田　岳

平成22年5月